Virologica Sinica 38 (2023) 631–634

Contents lists available at ScienceDirect

Virologica Sinica

journal homepage: www.keaipublishing.com/en/journals/virologica-sinica
www.virosin.org

Letter

Optimization and applications of an *in vivo* bioluminescence imaging model of influenza A virus infections

Xiaojing Lin [a,1], Murong Zhu [a,1], Xiujuan Zhao [a], Longlong Si [b], Meiyue Dong [a], Varada Anirudhan [c], Qinghua Cui [a,d,*], Lijun Rong [c,*], Ruikun Du [a,d,*]

[a] Innovative Institute of Chinese Medicine and Pharmacy, Shandong University of Traditional Chinese Medicine, Jinan, 50355, China
[b] CAS Key Laboratory of Quantitative Engineering Biology, Shenzhen Institute of Synthetic Biology, Shenzhen Institute of Advanced Technology, Chinese Academy of Sciences, Shenzhen, 518055, China
[c] Department of Microbiology and Immunology, College of Medicine, University of Illinois at Chicago, Chicago, IL 60612, USA
[d] Qingdao Academy of Chinese Medical Sciences, Shandong University of Traditional Chinese Medicine, Qingdao, 266122, China

Dear Editor,

In vivo bioluminescence imaging (BLI) models of virus infection possess unique advantages over conventional assays. For instance, the BLI model enables rapid and real-time detection of viral load and dissemination in the same animal over time (Mehle, 2015; Wen et al., 2022). A major hurdle to establish an *in vivo* BLI model of viral infection is the requirement of recombinant viruses encoding luciferases, as the reporter viruses are usually either genetically unstable or attenuated due to limited tolerance of viral genomes. Recently, we had generated two stable and replication-competent recombinant influenza A viruses (IAVs) carrying the firefly luciferase (*Fluc*) gene, including PR8-Fluc (H1N1; originally designated as PR8-NS^{CE2}-Fluc) and X31-Fluc (H3N2; originally designated as X31-NS^{CE2}-Fluc) viruses. Further, robust *in vivo* BLI models of both subtype H1N1 and H3N2 IAV infections were established based on the PR8-Fluc and X31-Fluc viruses, respectively (Zhao et al., 2022). In the present study, we used these advanced animal models to address several critical issues in both basic and applied influenza virology that have been of concern.

Nasal inoculation is usually adopted to establish mouse models of influenza virus infection, while the documented protocols to perform nasal inoculation are slightly different; the volume of virus stocks used to challenge mice ranges from 25 to 100 μL (Belser et al., 2013; Govorkova et al., 2001; Kandasamy et al., 2020). We herein questioned whether the divergence affected the efficacy of infection. To answer this, female BLAB/c mice (4–6 weeks old) were inoculated intranasally with a sub-lethal dose (1000 $TCID_{50}$) of the reporter PR8-Fluc virus in increasing volumes (10, 30, 50 and 100 μL) of sterile phosphate buffer saline (PBS). At day 1 post infection (p.i.), BLI was performed. It can be observed that the signals from the lung regions of mice became brighter as the inoculation volumes increased, indicating enhanced initial infection (Fig. 1A). In addition, the statistics of the bioluminescent signals clearly demonstrated that the efficacy of initial infection increased with increase in the nasal inoculation volumes (Fig. 1B). Notably, the bioluminescent signals from mice intranasally infected with 10 μL virus stocks generated an intragroup variation of as high as 0.68, signals from mice infected with 30 and 100 μL volumes generated comparable intragroup variations of 0.38 and 0.31 respectively, while signals from mice of 50 μL volume group showed the lowest intragroup variation of 0.15. Together, as intranasal inoculation of mice with IAVs in 50 μL stocks could guarantee a relatively high efficiency of initial infection and generate the lowest intragroup variation, we prefer using 50 μL over other volumes of virus stocks to infect mice intranasally in an optimized protocol.

Next, we adapted the BLI model as an advanced approach for rapid evaluation of influenza vaccines. Recently, our colleagues Si et al. (2022) had developed a novel live attenuated proteolysis-targeting chimeric (PROTAC) influenza vaccine (M1-PTD) based on the influenza A/WSN/33 (H1N1) virus. This vaccine can elicit robust and broad humoral, mucosal and cellular immunity in mice, promising protection against infections by both homologous and heterologous strains of subtype H1N1 (Si et al., 2022). We wanted to assess whether this PROTAC vaccine has the potency to broadly protect mice from infections of other IAV subtypes. For this purpose, female BLAB/c mice (4–6 weeks old) were intranasally vaccinated with the PROTAC vaccine M1-PTD at a dose of 10,000 $TCID_{50}$/mice. Mice inoculated with vehicles only were set as negative controls. At 28 days post vaccination, both control and vaccinated mice were challenged at a high dose (10,000 $TCID_{50}$) with the reporter PR8-Fluc (H1N1) and X31-Fluc (H3N2) viruses, respectively. At day 2 p.i., BLI was carried out to monitor the virus infection. As a result, upon infection with both PR8-Fluc and X31-Fluc viruses, only

* Corresponding authors.
E-mail addresses: cuiqinghua@sdutcm.edu.cn (Q. Cui), lijun@uic.edu (L. Rong), ruikun@sdutcm.edu.cn (R. Du).
[1] Xiaojing Lin and Murong Zhu contributed equally to this work.

https://doi.org/10.1016/j.virs.2023.04.007
Received 3 March 2023; Accepted 26 April 2023
Available online 2 May 2023

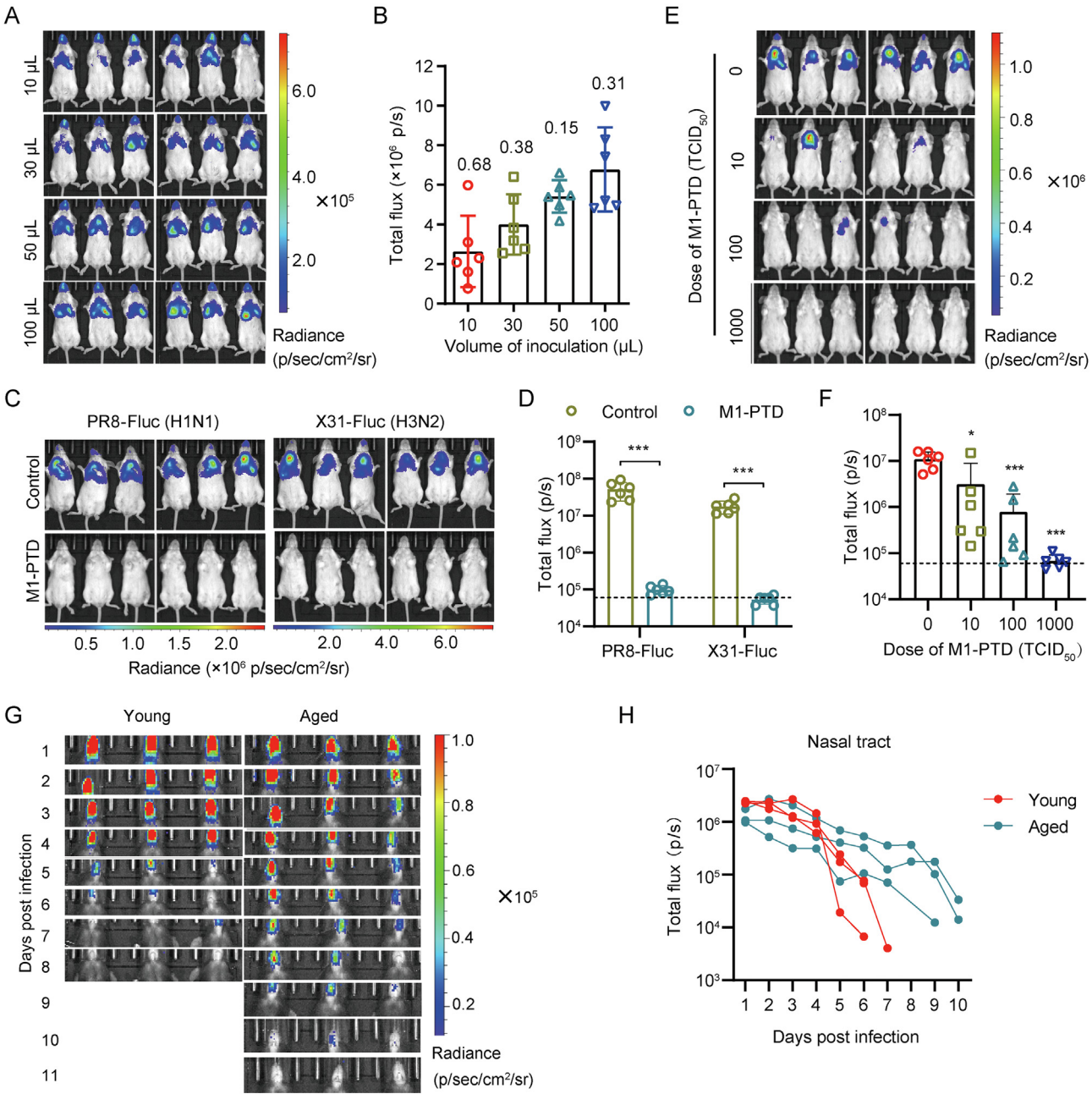

Figure 1. *In vivo* imaging assay of influenza virus infections in mice. **A, B** The dependence of viral infection on volumes of virus stocks used during nasal inoculation. Female BALB/c mice (4–6 weeks old) were inoculated intranasally with a sublethal dose (1000 $TCID_{50}$) of the reporter PR8-Fluc virus in increasing volumes ranged from 10 to 100 μL. Bioluminescence imaging (BLI) was performed at day 1 post infection (p.i.). The images and statistics of the BLI signals from lungs of the mice were shown in **(A)** and **(B)**, respectively. The intragroup variation values are shown on the top of columns. **C, D** Evaluation of an attenuated influenza vaccine using the BLI-based mouse model. Female BALB/c mice (4–6 weeks old) were mock treated or immunized with an attenuated influenza vaccine M1-PTD intranasally at a dose of 10,000 $TCID_{50}$/mice. At 28 days post vaccination, the mice were challenged with 10,000 $TCID_{50}$ of the reporter viruses PR8-Fluc (H1N1) and X31-Fluc (H3N2) separately. At day 2 p.i., BLI was performed **(C)** and the bioluminescence signals from lungs were analyzed **(D)**. **E, F** Dose-dependent immunization of the attenuated influenza vaccine M1-PTD. Female BALB/c mice (4–6 weeks old) were mock treated or immunized with M1-PTD intranasally at different doses of 10, 100 and 1000 $TCID_{50}$/mice separately. At 28 days post vaccination, the mice were challenged with 10,000 $TCID_{50}$ of the reporter viruses PR8-Fluc (H1N1). At day 2 p.i., BLI was performed **(E)** and the bioluminescence signals from lungs were analyzed **(F)**. **G, H** BLI-based kinetics of influenza A virus infection in aged mice. Groups of young (4–6 weeks old) and aged (18–20 months old) female C57BL/6 mice were infected with the reporter PR8-Fluc virus at a sublethal dose of 10,000 $TCID_{50}$, followed by BLI imaging every day. **G** Bioluminescence images acquired from the nasal tracts of infected mice. **H** The kinetics of bioluminescence from the nasal tract of each infected mouse. Dashed line indicates the background BLI signal. Error bars show the standard deviation (SD) of the mean from indicated replicates; *, $P < 0.05$; ***, $P < 0.001$; student's *t*-test.

bioluminescence signals at a level of background were collected from M1-PTD vaccinated mice, in contrast to the bright light observed from the control mice (Fig. 1C and D). These results indicate that M1-PTD confers complete protection against infection of both H1N1 and H3N2 subtype IAVs, implying its potential as a universal influenza vaccine (Du et al., 2021b).

To better evaluate the immunogenicity of M1-PTD, female BLAB/c mice (4–6 weeks old) were intranasally immunized with series doses of

M1-PTD at 10, 100, and 1000 $TCID_{50}$/mice, followed by virus challenge with the reporter PR8-Fluc virus (10,000 $TCID_{50}$) at 28 days post vaccination. Mock immunized mice were challenged in parallel as negative controls. At day 2 p.i., BLI was carried out to monitor virus infection. As shown in Fig. 1E, immunization of mice with M1-PTD induced dose-dependent protection from IAV infection. It was observed that a dose of 1000 $TCID_{50}$ M1-PTD provided complete protection from virus infection since only background bioluminescence was detected from all the immunized mice. While the mice receiving 100 and 10 $TCID_{50}$ doses of vaccination acquired partial protection. Although most of the mice got infected, the viral infection/spread were significantly restricted ($P < 0.001$ and $P < 0.05$ for the 100 and 10 $TCID_{50}$ doses respectively; Fig. 1F).

Besides the simplified detection of viral load in living animals using the *in vivo* BLI assay compared to conventional models, the number of animals required for a single experiment can be markedly reduced using the BLI model (Mehle, 2015); thus, the assay's throughput is relatively improved. These advances can further facilitate the development of novel influenza vaccines. For example, the BLI model allows rapid evaluation of a panel of candidate vaccines, or similarly, it can be used to screen optimized adjuvant for a selected influenza vaccine.

The advanced *in vivo* BLI model of IAV infections would also facilitate the development of novel antivirals. Previously, we had identified a novel IAV inhibitor CBS1194 that specifically targets group-2 influenza hemagglutinin proteins (Du et al., 2021a). In order to determine whether CBS1194 has the potential to prevent IAV infection *in vivo*, female BALB/c mice (4–6 weeks old) were infected with the reporter X31-Fluc (H3N2) at a sublethal dose of 1000 $TCID_{50}$, and treated with CBS1194 via intraperitoneal administration. As a result, neither low (25 mg/kg/day) nor high (100 mg/kg/day) dose of CBS1194 showed inhibition against IAV infection *in vivo*, while mice treated with oseltamivir phosphate (30 mg/kg/day) showed significantly decreased virus infection (Supplementary Figure S1). Despite the data are negative, our results suggested the potency of the BLI models for "*in vivo* screen" of novel antivirals.

Elderly individuals (>65 years) are at higher risks for mortality from IAV infection, bearing a disproportionate burden of illness, hospitalizations, and death (Iuliano et al., 2018; Talbot, 2017). It has been well acknowledged that the aging-associated immune-senescence limits the capacity to mount effective innate and adaptive immune response to virus infection, resulting in more severe disease (Chen et al., 2009). Nonetheless, lingering questions on the detailed pathogenesis of IAV infection in aged individuals remain elusive.

In order to better understand the aging-associated differences in the host response to influenza virus infection, both young (4–6 weeks old) and aged (18–20 months old) C57BL/6 mice (female, n = 3 mice/group) were infected with the reporter PR8-Fluc virus at a sublethal dose of 10,000 $TCID_{50}$, followed by daily BLI imaging to monitor the dynamics of IAV infection and dissemination *in vivo*. Unexpectedly, as all three young mice showed bright bioluminescence signals from lungs, suggesting successful establishment of virus infection, two of aged mice exhibited background signal while the third one emitted very weak light from its lungs (Supplementary Figure S2). This result demonstrates that the lungs of aged C57BL/6 mice are resistant to IAV infection. Previously, Liu et al. reported that aged C57BL/6 mice are more resistant to influenza virus infection (Lu et al., 2018), which is in consistent with our findings. However, Harris et al. have recently established an aged model of IAV infection using BALB/c mice and illustrated increased viral load and lung injury (Harris et al., 2021), which is contradictory to our results. We are unsure whether the difference in strains of mice used to establish the aged models attribute to the inconsistency between the two studies. Thus, further studies are required to establish an optimized mouse model of aging that better recapitulates human immune-senescence.

Interestingly, we noticed the prolonged detection of bioluminescence from regions corresponding to nasal tract in aged mice compared to young animals, as signals from young mice were almost completely eliminated at day 6 or 7 p.i., bioluminescence can be detected in aged mice till day 10 p.i., suggesting markedly delayed viral clearance (Fig. 1G). The kinetics of viral residence in nasal tract of each young and aged mice was dissected in Fig. 1H, and it clearly demonstrated the slower and delayed viral clearance in the upper respiratory tract of aged mice, which is in accordance to the impaired innate mucosal immunity associated with aging (Aso et al., 2016; Bates et al., 2008). Based on these observations, we can state that the *in vivo* BLI-based aged mouse model can provide a powerful tool to develop novel therapeutics or adjuvants that restore impaired mucosal immune responses in aged individuals (Aso et al., 2016; Bates et al., 2008).

To summarize, in the present study we applied the *in vivo* BLI model of IAV infections in both basic and applied influenza virology. Compared to conventional assays, the BLI models possess many unique advances, such as the real-time and longitudinal measurements of viral load in living animals, as well as improved throughput of the assay. The advanced BLI model calls for further utilization and will provide more powerful tools in the future.

Footnotes

This work was supported by the National Natural Science Foundation of China (82104134) and the Open Research Fund Program of the State Key Laboratory of Virology of China (2022IOV003). We thank Prof. Dongmei Qi and Dr. Xiwen Geng from the Experimental Center of Shandong University of Traditional Chinese Medicine for their technical support. Prof. Lijun Rong is an editorial board member for Virologica Sinica and was not involved in the editorial review or the decision to publish this article. The authors declare that they have no conflict of interest. All animal procedures were performed in accordance with protocols approved by the Institutional Animal Care and Use Committee (IACUC) of Shandong University of Traditional Chinese Medicine (Approval: SDUTCM20230213001).

Supplementary data to this article can be found online at https://doi.org/10.1016/j.virs.2023.04.007.

References

Aso, K., Tsuruhara, A., Takagaki, K., Oki, K., Ota, M., Nose, Y., Tanemura, H., Urushihata, N., Sasanuma, J., Sano, M., Hirano, A., Aso, R., McGhee, J.R., Fujihashi, K., 2016. Adipose-derived mesenchymal stem cells restore impaired mucosal immune responses in aged mice. PLoS One 11, e0148185.

Bates, J.T., Honko, A.N., Graff, A.H., Kock, N.D., Mizel, S.B., 2008. Mucosal adjuvant activity of flagellin in aged mice. Mech. Ageing Dev. 129, 271–281.

Belser, J.A., Gustin, K.M., Pearce, M.B., Maines, T.R., Zeng, H., Pappas, C., Sun, X., Carney, P.J., Villanueva, J.M., Stevens, J., Katz, J.M., Tumpey, T.M., 2013. Pathogenesis and transmission of avian influenza A (H7N9) virus in ferrets and mice. Nature 501, 556–559.

Chen, W.H., Kozlovsky, B.F., Effros, R.B., Grubeck-Loebenstein, B., Edelman, R., Sztein, M.B., 2009. Vaccination in the elderly: an immunological perspective. Trends Immunol. 30, 351–359.

Du, R., Cheng, H., Cui, Q., Peet, N.P., Gaisina, I.N., Rong, L., 2021a. Identification of a novel inhibitor targeting influenza A virus group 2 hemagglutinins. Antivir. Res. 186, 105013.

Du, R., Cui, Q., Rong, L., 2021b. Flu universal vaccines: new tricks on an old virus. Virol. Sin. 36, 13–24.

Govorkova, E.A., Leneva, I.A., Goloubeva, O.G., Bush, K., Webster, R.G., 2001. Comparison of efficacies of RWJ-270201, zanamivir, and oseltamivir against H5N1, H9N2, and other avian influenza viruses. Antimicrob. Agents Chemother. 45, 2723–2732.

Harris, R., Yang, J., Pagan, K., Cho, S.J., Stout-Delgado, H., 2021. Antiviral gene expression in young and aged murine lung during H1N1 and H3N2. Int. J. Mol. Sci. 22, 12097.

Iuliano, A.D., Roguski, K.M., Chang, H.H., Muscatello, D.J., Palekar, R., Tempia, S., Cohen, C., Gran, J.M., Schanzer, D., Cowling, B.J., Wu, P., Kyncl, J., Ang, L.W., Park, M., Redlberger-Fritz, M., Yu, H., Espenhain, L., Krishnan, A., Emukule, G., van Asten, L., Pereira da Silva, S., Aungkulanon, S., Buchholz, U., Widdowson, M.A., Bresee, J.S., 2018. Estimates of global seasonal influenza-associated respiratory mortality: a modelling study. Lancet 391, 1285–1300.

Kandasamy, M., Furlong, K., Perez, J.T., Manicassamy, S., Manicassamy, B., 2020. Suppression of cytotoxic T cell functions and decreased levels of tissue-resident memory T cells during H5N1 infection. J. Virol. 94, e00057–20.

Lu, J., Duan, X., Zhao, W., Wang, J., Wang, H., Zhou, K., Fang, M., 2018. Aged mice are more resistant to influenza virus infection due to reduced inflammation and lung pathology. Aging Dis 9, 358–373.

Mehle, A., 2015. Fiat luc: bioluminescence imaging reveals in vivo viral replication dynamics. PLoS Pathog. 11, e1005081.
Si, L., Shen, Q., Li, J., Chen, L., Shen, J., Xiao, X., Bai, H., Feng, T., Ye, A.Y., Li, L., Zhang, C., Li, Z., Wang, P., Oh, C.Y., Nurani, A., Niu, S., Zhang, C., Wei, X., Yuan, W., Liao, H., Huang, X., Wang, N., Tian, W.X., Tian, H., Li, L., Liu, X., Plebani, R., 2022. Generation of a live attenuated influenza A vaccine by proteolysis targeting. Nat. Biotechnol. 40, 1370–1377.
Talbot, H.K., 2017. Influenza in older adults. Infect. Dis. Clin. 31, 757–766.
Wen, X., Zhang, L., Liu, Q., Xiao, X., Huang, W., Wang, Y., 2022. Screening and identification of HTNV(pv) entry inhibitors with high-throughput pseudovirus-based chemiluminescence. Virol. Sin. 37, 531–537.
Zhao, X., Lin, X., Li, P., Chen, Z., Zhang, C., Manicassamy, B., Rong, L., Cui, Q., Du, R., 2022. Expanding the tolerance of segmented Influenza A Virus genome using a balance compensation strategy. PLoS Pathog. 18, e1010756.